JOURNAL OF MATERIALS SCIENCE **32** (1997) 91–97

Reaction and diffusion path of an interface reaction between Cu_2O and nickel

H. INABA
Technical Research Laboratories, Kawasaki Steel Corporation, 1 Kawasaki-Chou, Chuo-Ku, Chiba, 260, Japan

The interface reaction between Cu_2O and nickel has been investigated and the reaction path has been analysed on the chemical potential diagram for undoped and doped samples. The layer sequence of products Cu_2O/Cu/NiO/Ni for the undoped sample and that of Cu_2O/Cu/NiO/Cu–Ni alloy/Ni for the doped sample was obtained. The reaction and diffusion path was explained on the chemical potential diagram of the Cu–Ni–O system, based on the assumption that a local equilibrium is attained at the interfaces. The doping effect of NiO in Cu_2O was ascribed to a higher mobility of copper in NiO phase due to the higher chemical potential of oxygen at the Cu/NiO interface resulting from the higher chemical potential of nickel in Cu_2O. When the reaction time becomes longer, it is expected that the reaction and diffusion path will become similar to that of the doped sample. Because the reaction and diffusion path is a function of time and has a non-equilibrium character, it can be represented and reasonably explained on the chemical potential diagram obtained from a thermodynamic treatment.

1. Introduction

The analysis of the interface reaction has become increasingly important, not only in the area of basic solid-state chemistry but also in the development of materials, such as diffusion bonding, surface coating, the multi-component grain boundary in ceramics, composite materials and oxidation of alloys. Various kinds of interface reactions, such as the displacement reaction ($A + BX = B + AX$) [1–3], internal oxidation in non-metallic solid solutions [4], kinetic demixing and decomposition [5] and metal/non-metal reactions [6–9] have been extensively investigated. In order to analyse the multi-component interface reactions, the considerations of not only thermodynamics but also diffusion for multi-component systems, are necessary.

Yokokawa *et al.* [6–8] have proposed the use of a chemical potential diagram to analyse the multi-component interface reactions, because the driving force of chemical reaction and diffusion is the gradient of chemical potential. They have successfully elucidated the order of phases formed by the interface reaction by the use of multi-component chemical potential diagrams, assuming a local equilibrium in the interfaces. However, it has still not been clearly shown through which part of the chemical potential diagram the reaction path passes during the reaction, nor the mechanism to determine the reaction and diffusion path.

Rapp *et al.* [1] investigated the displacement reaction between Cu_2O and nickel and found that it formed the layer sequence of Cu_2O/Cu/NiO/Ni. They made a theoretical analysis for the purpose of predicting the morphologies and reaction rates from a knowledge of thermodynamic and diffusion data, based on a modification of Wagner's theory of oxidation kinetics [10]. Loo *et al.* [2, 3] elucidated the reason for determining the sequence A/AX/B/BX or A/B/AX/BX in the displacement reaction ($A + BX = B + AX$) by considering the tie-lines between metal phases and the phases of AX and BX. Vosters *et al.* [11] investigated the impurity effect on the displacement reaction between nickel and Cu_2O and found that the morphology changed when Cu_2O was contaminated with chlorine.

In this study, the interface reaction between Cu_2O and nickel for undoped and doped Cu_2O samples with NiO has been investigated and the reaction and diffusion path has been analysed on the chemical potential diagram for the Cu–Ni–O system for undoped and doped samples.

2. Experimental procedure

A nickel sheet with 99.99% purity and a thickness of 1 mm, and CuO powder with 99.9% purity, were provided for the Cu_2O and nickel couple. The CuO powder was reduced to Cu_2O under a nitrogen gas flow with an oxygen partial pressure of 2×10^{-5} atm at 1273 K. For doped samples, NiO powder was mixed with CuO powder in an agate mortar in appropriate ratios, in order to obtain the molar ratios of NiO/Cu_2O: 0.01, 0.02, 0.05 and 0.1. The doped CuO powder was reduced to doped Cu_2O in an oxygen partial pressure of 2×10^{-5} atm at 1273 K for most samples and for 0.01 mol NiO/Cu_2O in oxygen

0022–2461 © *1997 Chapman & Hall*

partial pressures of 2×10^{-5}, 2×10^{-4}, 2×10^{-3} and 2×10^{-2} atm at 1273 K. The oxygen partial pressures were obtained by controlling the ratio of the flowing gas mixture of oxygen and nitrogen using mass flow controllers. The X-ray diffractometry was conducted for undoped and doped Cu_2O in order to determine the lattice parameter and phases. The undoped and doped diffusion couples of Ni/Cu_2O were pressed in a stainless steel cylinder, similar to that described by Laheij *et al.* [12], where the sample was automatically sealed during the heating process of annealing. The diffusion couples were annealed at 1273 K for various periods of time. The profiles of copper, nickel and oxygen atoms after the reaction were analysed using an electron probe microanalyser (EPMA). The line-analysis of EPMA was carried out with the voltage of 15 kV, beam current of 50 nA, beam diameter of about 1 μm and a scan speed of 50 $\mu m\,min^{-1}$.

3. Results

The lattice parameter was found to be 0.42693 ± 0.00002 nm for both undoped and doped Cu_2O. Nickel oxide phase was detected for doped Cu_2O, and CuO phase was also detected for the sample of Cu_2O made in an oxygen partial pressure of 2×10^{-3} atm. These facts mean that NiO does not dissolve in the Cu_2O lattice significantly, and the doped NiO is present mostly as NiO in Cu_2O. These results are compatible with the e.m.f. study [13] of the Cu–Cu_2O–NiO system, where the solubility of nickel in Cu_2O was observed to be only 0.9 at %.

The results for the doped Cu_2O (0.01 mol NiO)/Ni couple after reaction at 1273 K showed a layered structure similar to the results by Rapp *et al.* [1]. The thicknesses of the layers of copper and NiO for the doped Cu_2O (0.01 mol NiO)/Ni were measured and are plotted against square root of reaction time in Fig. 1, where the linear relationship is seen to be as observed for the undoped diffusion couple by Rapp *et al.* [1]. This linear relationship suggests that the displacement reaction is controlled by diffusion and the steady state is attained in the main reaction. However, the total reaction would not be in a steady state, as will be discussed in the next section.

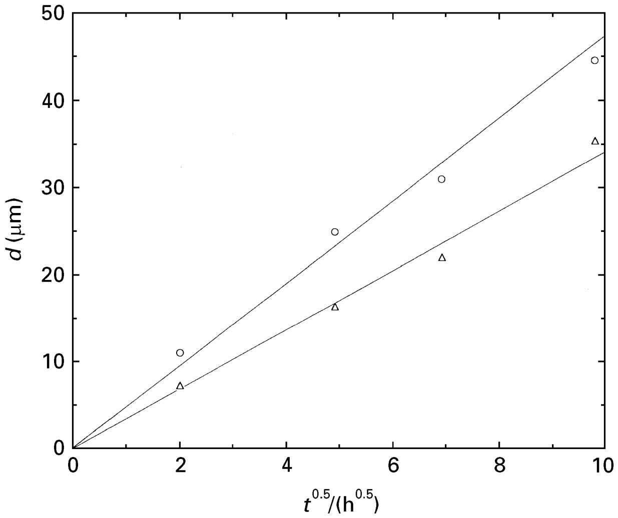

Figure 1 The thickness of the layers of (○) copper and (△) NiO for the doped Cu_2O (0.01 mol NiO)/Ni against square root of reaction time.

The rate constant of copper, $k_p'(Cu)$, is calculated from the slope of the linear plot to be $3.0\times10^{-11}\ cm^2\,s^{-1}$, which is considerably higher than that of the undoped sample obtained by Rapp *et al.* [1], $1.7\times10^{-11}\ cm^2\,s^{-1}$. The larger value obtained in this study is considered to be due to the doping effect of NiO in Cu_2O. The mechanism whereby the rate constant is higher in the doped system is considered to be due to the higher mobility of nickel in the NiO phase, because the rate of the displacement reaction is determined by the diffusion of nickel in the NiO phase and the reaction path for the doped case passes through a higher oxidation–potential area on the chemical potential diagram in the NiO phase, as will be discussed in the next section. The molar ratio of product layers between copper and NiO calculated from the thickness was about 2 within experimental error. Because the diffusion constant of oxygen in the copper phase is several orders of magnitude larger than that of nickel in the NiO phase, this fact supports the conclusion that the displacement reaction is controlled by the diffusion of nickel in the NiO phase, as described by Rapp *et al.* [1].

The results of the EPMA analysis after the reactions of undoped and doped Cu_2O/Ni couples are shown in Fig. 2. As seen in Fig. 2, a Cu–Ni alloy phase was formed significantly between NiO and nickel phases when Cu_2O was doped with NiO. The concentration of copper in Cu–Ni alloy was increased, when the doped amount of NiO was increased. It should be noted here that even in the undoped sample, copper diffuses in the NiO phase towards the Ni/NiO interface, and can be seen as a small content of copper at the Ni/NiO interface in Fig. 2(a). The compositional analysis of copper and nickel phases for undoped and doped (0.1 mol NiO) Cu_2O/Ni couples was made by EPMA after the calibration using pure copper and nickel metals and sintered Cu_2O and NiO discs. The results are listed in Table I. As seen in Table I, there is no significant difference in the composition of the nickel phase between undoped and doped couples, but the concentration of nickel and oxygen of the copper phase of the doped couple is significantly larger than that of the undoped couple.

4. Discussion

4.1. Construction of a chemical potential diagram

As has been described by Yokokawa *et al.* [6–8], the use of a chemical potential diagram is very useful in order to interpret multi-component interface reactions. The chemical potential diagram of the Cu–Ni–O system has been constructed as follows [6–8]. We consider a compound of $Cu_{ki}Ni_{li}O_{mi}$, which is the general form of the compound composed

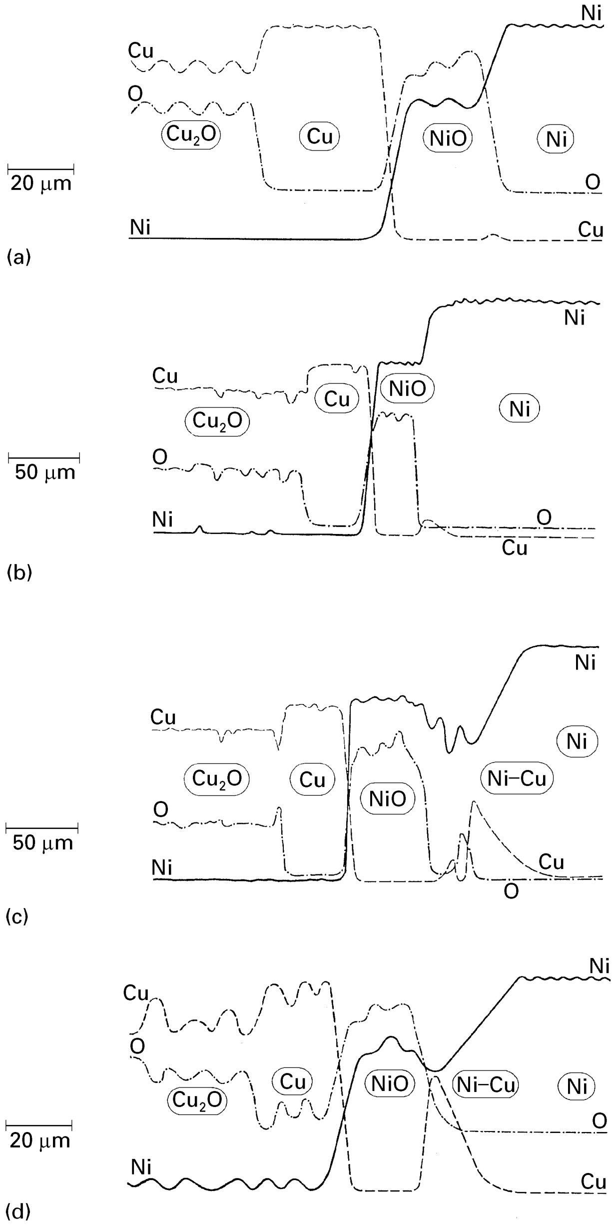

Figure 2 The results of the EPMA analysis after the reaction for 96 h at 1273 K for undoped and doped Cu_2O/Ni couples: (a) undoped, (b) 0.01 mol NiO doped, (c) 0.02 mol NiO doped, (d) 0.1 mol NiO doped.

TABLE I EPMA analysis of nickel and copper phases for the diffusion couples of Cu_2O/Ni using Cu_2O undoped and doped with NiO after annealing for 96 h at 1273 K

	Phase	Composition
Cu_2O undoped	Ni phase	$Ni_{0.989}Cu_{0.001}O_{0.010}$
	Cu phase	$Cu_{0.944}Ni_{0.004}O_{0.052}$
Cu_2O doped with 0.1 mol NiO	Ni phase	$Ni_{0.988}Cu_{0.000}O_{0.012}$
	Cu phase	$Cu_{0.848}Ni_{0.036}O_{0.116}$

of copper, nickel and oxygen, and calculate the chemical potential of each component, μ_i, when the three phases of the compound coexist. Consider the following reaction

$$ki\,\mathrm{Cu} + li\,\mathrm{Ni} + mi\,\mathrm{O} = \mathrm{Cu}_{ki}\mathrm{Ni}_{li}\mathrm{O}_{mi} \qquad (1)$$

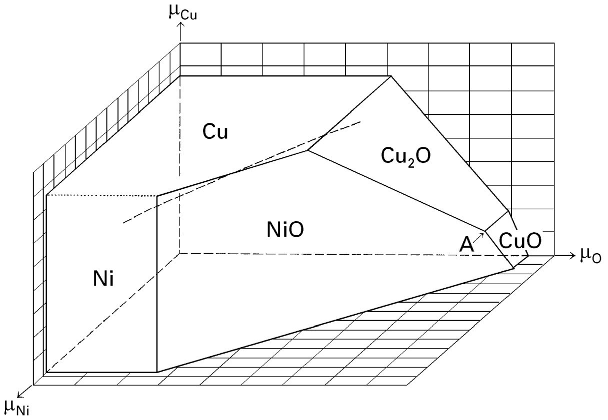

Figure 3 Three-dimensional chemical potential diagram of Cu–Ni–O system at 1273 K. The chemical potential of coexisting CuO, Cu_2O and NiO phases is marked A. The broken line shows a supposed reaction path for the interface reaction between Cu_2O and nickel.

then the chemical potential of the compound can be represented by the sum of each component as

$$\mu(\mathrm{Cu}_{ki}\mathrm{Ni}_{li}\mathrm{O}_{mi}) = ki\mu(\mathrm{Cu}) + li\mu(\mathrm{Ni}) + mi\mu(\mathrm{O}) \qquad (2)$$

Because the chemical potential of a phase *i* is equal to the Gibbs energy of the formation of the phase *i*, we obtain

$$\mu(\mathrm{phase}_i) = \Delta_f G^0\ (\mathrm{phase}_i) \qquad (3)$$

When we apply Equation 3 to the chemical potential of coexisting CuO, Cu_2O and NiO phases as an example, we obtain

$$\mu(\mathrm{Cu_{CuO}}) + \mu(\mathrm{O_{CuO}}) = \Delta_f G^0(\mathrm{CuO}) \qquad (4)$$

$$2\mu(\mathrm{Cu_{Cu_2O}}) + \mu(\mathrm{O_{Cu_2O}}) = \Delta_f G^0(\mathrm{Cu_2O}) \qquad (5)$$

$$\mu(\mathrm{Ni_{NiO}}) + \mu(\mathrm{O_{NiO}}) = \Delta_f G^0(\mathrm{NiO}) \qquad (6)$$

where μ (M_i) is the chemical potential of M in the phase *i*.

Because these three phases coexist, we have

$$\mu(\mathrm{Cu_{CuO}}) = \mu(\mathrm{Cu_{Cu_2O}}) \qquad (7)$$

$$\mu(\mathrm{O_{CuO}}) = \mu(\mathrm{O_{Cu_2O}}) = \mu(\mathrm{O_{NiO}}) \qquad (8)$$

Then Equations 4–6 can be solved, because we have the values of $\Delta_f G^0$ (phase$_i$) from the thermodynamic database of MALT2, and we only have the three unknown parameters μ(Cu), μ(O) and μ(Ni). Applying Equation 3 to all possible phases composed of the Cu–Ni–O system, we can construct a three-dimensional chemical potential diagram, which for 1273 K is shown in Fig. 3. The chemical potential of coexisting CuO, Cu_2O and NiO phases is marked as A in Fig. 3. It should be noted here that copper and nickel form a complete solid solution at this temperature, but we regard copper and nickel as separate phases here for the sake of convenience and draw a dotted line on the boundary between the hypothetical separate phases as shown in Fig. 3. The reason why we regard copper and nickel as separate phases is that this diagram is true and convenient to analyse the reaction and diffusion path when copper does not contact with nickel.

4.2. Analysis of the interface reaction using the chemical potential diagram

The understanding of the resultant layered sequence Cu_2O/Cu/NiO/Ni may not be straightforward, because the metallic phase of copper is formed between two oxide phases, and the oxide phase of NiO is formed between two metallic phases. It can, however, be easily understood by drawing a broken line on the chemical potential diagram, as shown in Fig. 3, and thinking that the reaction and diffusion pass along this line on the chemical potential diagram. The following assumptions have been made for the analysis of phase reactions by using the chemical potential diagram.

1. The local equilibrium is attained at the interfaces, although the whole system is under a non-equilibrium condition.
2. There is no kinetic barrier, such as the chemical reaction at the interface and nucleation.
3. The reaction follows a path so as to maintain materials balance.
4. The driving force of reaction and diffusion is the gradient of chemical potentials, and the reaction and diffusion path follows the diffusion equation in each phase.
5. The reaction path is generally dependent on the thickness of the sample and time of the reaction.

The mechanism of the displacement reaction for Cu_2O/Ni is considered to be described as follows. At the Cu_2O/Cu interface, cuprous oxide decomposes into copper and atomic oxygen. The oxygen atom diffuses through the copper phase towards the NiO phase, because the chemical potential of oxygen in the copper phase is considered to be larger than that in the NiO phase (see Figs 3 or 5). At the Ni/NiO interface, the nickel atom is oxidized to form a Ni^{2+} ion and two electrons, which diffuse through the NiO phase towards the copper phase. (Actually, positive holes diffuse through the NiO phase towards the Ni/NiO interface instead of electrons.) At the Cu/NiO interface, the oxygen atom, Ni^{2+} ion and two electrons meet to form NiO. The reaction and diffusion model for the displacement reaction is shown in Fig. 4a. However, the total reaction cannot be described by the displacement reaction only. Because the chemical potential gradient of copper exists in NiO and nickel phases, copper diffuses through the NiO and nickel phases. Similarly, nickel diffuses through the copper and Cu_2O phases. The diffusion model due to the chemical potential gradient, in addition to the displacement reaction, is shown in Fig. 4b. The formation of Cu–Ni alloy at the interface between Ni/NiO for the doped Cu_2O/Ni couple as shown in Fig. 2, can be understood as the result of the diffusion of copper through the NiO phase.

The difference in the reaction path between undoped and doped Cu_2O/Ni couples is considered to be as follows. The chemical potential of nickel in the Cu_2O phase of the doped sample is higher than that of the undoped one. Because there was no difference in the lattice parameter between undoped and doped samples and the existence of NiO was confirmed in the doped Cu_2O from X-ray diffraction, the solubility of NiO in Cu_2O is considered to be very slight, and the higher chemical potential of nickel of the doped sample should be taken as an average in the Cu_2O phase. The fact that there was no significant difference in product layers between Cu_2O made at various oxygen partial pressures shows that the chemical potential of nickel rather than that of oxygen in Cu_2O is important for the overall reaction path. The higher chemical potential of nickel of the doped sample may be kept until the Cu/NiO interface, but it would be reversed somewhere in the NiO phase, because Cu–Ni alloy is formed at the Ni/NiO interface. From these considerations, we can estimate the reaction and diffusion path for the undoped and doped samples on the chemical potential diagram of the Cu–Ni–O system, as shown schematically in Fig. 5. It is noted in Fig. 5 that the chemical potentials of nickel and oxygen in the copper phase for the doped sample are higher than those of the undoped one. Indeed the contents of nickel and oxygen in the copper phase for the doped sample are higher than those of the undoped ones according to the compositional analysis shown in Table I. The content of oxygen in the copper phase seems to be larger than the equilibrium solubility of about 0.3 at % found by Narula *et al.* [14], but it is probably due to a metastable oxide like $Cu_4O_{0.75}$, which was detected by electron microscopy by Guan *et al.* [15] in the sample of initial oxidation.

The diffusion path on the chemical potential diagram for the undoped and doped samples may be

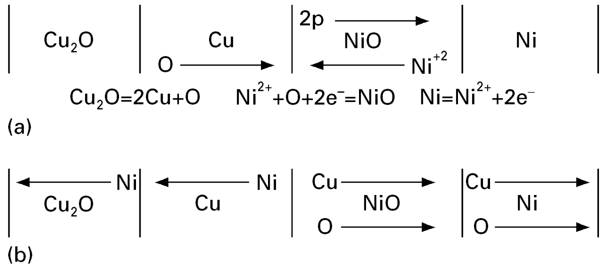

Figure 4 The reaction and diffusion model for the interface reaction between Cu_2O and nickel: (a) main interface reaction, (b) successive diffusion.

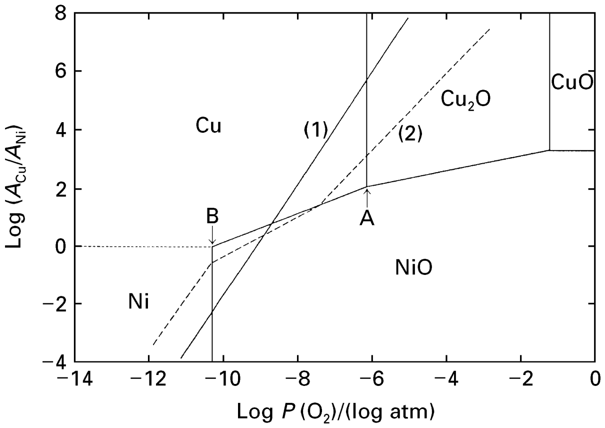

Figure 5 The estimated reaction and diffusion path on the chemical potential diagram for the interface reaction between Cu_2O and nickel with and without doping of NiO in Cu_2O. (1) (——) An undoped case, (2) (– – –) doped case.

understood using the diffusion equation derived using irreversible thermodynamics according to Kirkaldy and Young [16] as follows. The flux, J, of the component i in the phase k is expressed as

$$J_i^k = \sum_{j=1}^{n} L_{ij}^k(-\text{grad}\,\eta_j) \tag{9}$$

where η_j is the electrochemical potential of component j and L_{ij} is the mobility coefficient of component i due to the electrochemical potential gradient of component j. For the ionic phases such as NiO and Cu_2O, based on the assumption of site conservation, electrical neutrality condition and equilibrium equations relating the different components and defect species, it is possible to simplify Equation 9 into Equation 10 using the chemical potential instead of the electrochemical potential as

$$J_i^k = \sum_{j=1}^{n} L_{ij}^k(-\text{grad}\,\mu_j) \tag{10}$$

Because Equation 10 can also be applied to the metallic phases, the fluxes of copper, nickel and oxygen atoms in copper and NiO phases are written as

$$J_{\mathrm{Cu}}^{\mathrm{Cu}} = -L_{\mathrm{CuCu}}^{\mathrm{Cu}}\frac{\partial\mu_{\mathrm{Cu}}}{\partial x} - L_{\mathrm{CuNi}}^{\mathrm{Cu}}\frac{\partial\mu_{\mathrm{Ni}}}{\partial x} - L_{\mathrm{CuO}}^{\mathrm{Cu}}\frac{\partial\mu_{\mathrm{O}}}{\partial x} \tag{11}$$

$$J_{\mathrm{Ni}}^{\mathrm{Cu}} = -L_{\mathrm{NiCu}}^{\mathrm{Cu}}\frac{\partial\mu_{\mathrm{Cu}}}{\partial x} - L_{\mathrm{NiNi}}^{\mathrm{Cu}}\frac{\partial\mu_{\mathrm{Ni}}}{\partial x} - L_{\mathrm{NiO}}^{\mathrm{Cu}}\frac{\partial\mu_{\mathrm{O}}}{\partial x} \tag{12}$$

$$J_{\mathrm{O}}^{\mathrm{Cu}} = -L_{\mathrm{OCu}}^{\mathrm{Cu}}\frac{\partial\mu_{\mathrm{Cu}}}{\partial x} - L_{\mathrm{ONi}}^{\mathrm{Cu}}\frac{\partial\mu_{\mathrm{Ni}}}{\partial x} - L_{\mathrm{OO}}^{\mathrm{Cu}}\frac{\partial\mu_{\mathrm{O}}}{\partial x} \tag{13}$$

$$J_{\mathrm{Cu}}^{\mathrm{NiO}} = -L_{\mathrm{CuCu}}^{\mathrm{NiO}}\frac{\partial\mu_{\mathrm{Cu}}}{\partial x} - L_{\mathrm{CuNi}}^{\mathrm{NiO}}\frac{\partial\mu_{\mathrm{Ni}}}{\partial x} - L_{\mathrm{CuO}}^{\mathrm{NiO}}\frac{\partial\mu_{\mathrm{O}}}{\partial x} \tag{14}$$

$$J_{\mathrm{Ni}}^{\mathrm{NiO}} = -L_{\mathrm{NiCu}}^{\mathrm{NiO}}\frac{\partial\mu_{\mathrm{Cu}}}{\partial x} - L_{\mathrm{NiNi}}^{\mathrm{NiO}}\frac{\partial\mu_{\mathrm{Ni}}}{\partial x} - L_{\mathrm{NiO}}^{\mathrm{NiO}}\frac{\partial\mu_{\mathrm{O}}}{\partial x} \tag{15}$$

$$J_{\mathrm{O}}^{\mathrm{NiO}} = -L_{\mathrm{OCu}}^{\mathrm{NiO}}\frac{\partial\mu_{\mathrm{Cu}}}{\partial x} - L_{\mathrm{ONi}}^{\mathrm{NiO}}\frac{\partial\mu_{\mathrm{Ni}}}{\partial x} - L_{\mathrm{OO}}^{\mathrm{NiO}}\frac{\partial\mu_{\mathrm{O}}}{\partial x} \tag{16}$$

If these L_{ij} values were known for undoped and doped samples and using the boundary condition, these equations could be solved and the diffusion paths on the chemical potential might be determined. However, it is not possible to know these constants and to determine the diffusion paths quantitatively. Therefore, let us try to examine these constants and to understand the diffusion paths qualitatively. Generally, the off-diagonal terms are small compared with the diagonal terms, so that we have the following equations as a first approximation

$$J_{\mathrm{Cu}}^{\mathrm{Cu}} = -L_{\mathrm{CuCu}}^{\mathrm{Cu}}\frac{\partial\mu_{\mathrm{Cu}}}{\partial x} \tag{17}$$

$$J_{\mathrm{Ni}}^{\mathrm{Cu}} = -L_{\mathrm{NiNi}}^{\mathrm{Cu}}\frac{\partial\mu_{\mathrm{Ni}}}{\partial x} \tag{18}$$

$$J_{\mathrm{O}}^{\mathrm{Cu}} = -L_{\mathrm{OO}}^{\mathrm{Cu}}\frac{\partial\mu_{\mathrm{O}}}{\partial x} \tag{19}$$

$$J_{\mathrm{Cu}}^{\mathrm{NiO}} = -L_{\mathrm{CuCu}}^{\mathrm{NiO}}\frac{\partial\mu_{\mathrm{Cu}}}{\partial x} \tag{20}$$

$$J_{\mathrm{Ni}}^{\mathrm{NiO}} = -L_{\mathrm{NiNi}}^{\mathrm{NiO}}\frac{\partial\mu_{\mathrm{Ni}}}{\partial x} \tag{21}$$

$$J_{\mathrm{O}}^{\mathrm{NiO}} = -L_{\mathrm{OO}}^{\mathrm{NiO}}\frac{\partial\mu_{\mathrm{O}}}{\partial x} \tag{22}$$

Because the displacement reaction is controlled by the diffusion of nickel in NiO and considering the materials balance at the NiO/Cu interface, we obtain

$$J_{\mathrm{Ni}}^{\mathrm{NiO}} = -L_{\mathrm{NiNi}}^{\mathrm{NiO}}\frac{\partial\mu_{\mathrm{Ni}}}{\partial x} = J_{\mathrm{O}}^{\mathrm{Cu}} = -L_{\mathrm{OO}}^{\mathrm{Cu}}\frac{\partial\mu_{\mathrm{O}}}{\partial x} \tag{23}$$

Because $L_{\mathrm{OO}}^{\mathrm{Cu}} \gg L_{\mathrm{NiNi}}^{\mathrm{NiO}}$ according to Rapp *et al.* [1], the gradient of chemical potential of nickel in NiO is much smaller than that of oxygen in the copper phase.

The slope of the diffusion path of each phase on the chemical potential diagram shown in Fig. 5 is represented as

$$\left(\frac{\partial\mu_{\mathrm{Cu}}}{\partial x} - \frac{\partial\mu_{\mathrm{Ni}}}{\partial x}\right)\bigg/\frac{\partial\mu_{\mathrm{O}}}{\partial x} = \left(\frac{J_{\mathrm{Cu}}}{L_{\mathrm{CuCu}}} - \frac{J_{\mathrm{Ni}}}{L_{\mathrm{NiNi}}}\right)\bigg/\frac{J_{\mathrm{O}}}{L_{\mathrm{OO}}} \tag{24}$$

Generally speaking, the system is not in a steady state, so that the fluxes J_{Cu}, J_{Ni} and J_{O} are dependent on the position of the phase. The slope of the diffusion path of each phase on the chemical potential diagram is, therefore, dependent on the position of the phase and the diffusion path would not be expressed by a line in general. However, because the profiles of copper, nickel and oxygen atoms are similar during the reaction time studied, and the layer thickness is proportional to the square root of the reaction time, the total reaction and diffusion can be regarded to be in a steady state as an approximation. Therefore, the slope represented by Equation 24 is regarded as a constant, and the reaction and diffusion path is represented by the lines connected at the interface as an approximation, as shown in Fig. 5. The diffusion problems of multi-component systems with interfaces were treated by Kirkaldy [17, 18].

The estimation of L_{CuCu}, L_{NiNi} and L_{OO} in the copper phase for doped and undoped cases is not possible at present, because we do not have available data in such conditions. The estimation of L_{CuCu}, L_{NiNi} and L_{OO} in the NiO phase for doped and undoped cases is most important in order to analyse the interface reaction, because the displacement reaction is controlled by the diffusion of nickel in NiO and the chemical potential gradients of the undoped and doped sample are expected to cross at some point in NiO as shown in Fig. 5. The defect structure of NiO can be described using the Kröger and Vink notation according to Peterson and Wiley [19] as

$$1/2\mathrm{O}_2 = \mathrm{O}^{\mathrm{x}} + \mathrm{V}' + \mathrm{h}^{\cdot} \tag{25}$$

$$\mathrm{V}' = \mathrm{V}'' + \mathrm{h}^{\cdot} \tag{26}$$

where O^{x}, V', V'' and $\mathrm{h}^{\cdot}$ are a neutral oxygen, a singly charged cation vacancy, a doubly charged cation vacancy and an electron hole, respectively. When V' is the predominant defect for the cation vacancy, then we obtain

$$[\mathrm{V}'] = K_1 P(\mathrm{O}_2)^{1/4} \tag{27}$$

where $P(\mathrm{O}_2)$ is the partial pressure of oxygen and K_1 is a proportional constant. Similarly, when V″ is the predominant defect for the cation vacancy, we obtain

$$[\mathrm{V}''] = K_2 P(\mathrm{O}_2)^{1/6} \tag{28}$$

where K_2 is a proportional constant. The self-diffusion of nickel in NiO can be represented according to Peterson and Wiley [19] by

$$D_{\mathrm{Ni}} = D_{\mathrm{V}'} f_{\mathrm{v}} [\mathrm{V}'] + D_{\mathrm{V}''} f_{\mathrm{v}} [\mathrm{V}''] \tag{29}$$

where $D_{\mathrm{V}'}$, $D_{\mathrm{V}''}$ and f_{v} are the uncorrelated diffusion constants due to V′ and V″ and a constant depending on crystal geometry, respectively. They explained experimental data using Equation 29 and unequal contributions of V′ and V″. Because f_{v} is a constant of 0.781 and [V′] and [V″] are increasing functions with respect to $P(\mathrm{O}_2)$, D_{Ni} is also considered to be an increasing function with respect to $P(\mathrm{O}_2)$. It can be concluded that $L_{\mathrm{NiNi}}^{\mathrm{NiO}}$ is an increasing function with respect to $P(\mathrm{O}_2)$, because $L_{\mathrm{NiNi}}^{\mathrm{NiO}}$ is considered to be proportional to D_{Ni}. As can be seen in Fig. 5, the chemical potential of oxygen at the Cu/NiO interface for the doped sample is higher than that of the undoped one and therefore $L_{\mathrm{NiNi}}^{\mathrm{NiO}}$ of the doped sample is considered to be higher than that of the undoped one. This consideration is supported by the fact that the rate of growth of the product layers of copper and NiO for the doped sample is significantly higher than that for the undoped one.

Cation impurity diffusion in NiO has been measured by many investigators [20, 21] and it has been shown that the larger ions diffuse more rapidly and have a smaller activation energy than do smaller ions for transition-metal impurity ions having the same valence. Impurity diffusion of copper in NiO has not yet been measured, but it is considered to diffuse similarly via a vacancy mechanism. Thus $L_{\mathrm{CuCu}}^{\mathrm{NiO}}$ is also considered to be an increasing function with respect to $P(\mathrm{O}_2)$ and $L_{\mathrm{CuCu}}^{\mathrm{NiO}}$ of the doped sample is higher than that of the undoped one. Therefore, it is concluded that the diffusion path of the doped sample on the chemical potential diagram in a way as shown in Fig. 5, is mainly due to the larger mobility terms of copper and nickel in NiO phase.

It should be noted here that, even in the undoped sample, copper diffuses in the NiO phase towards the Ni/NiO interface, and can be seen as a small content of copper at the Ni/NiO interface in Fig. 2a. The content of copper at the Ni/NiO interface would be larger as the reaction time is longer. The doping effect can be regarded as the stimulating effect of the reaction due to the larger mobility term of copper and nickel in the NiO phase. When the reaction time becomes longer, the reaction and diffusion path is considered to be a similar one as the doped sample. If the reaction time is taken to be infinite using a semi-infinite size of sample, the reaction and diffusion path would approach the line A–B shown in Fig. 5, which is the nearest distance between $\mathrm{Cu_2O}$ and nickel phases on the chemical potential diagram. Thus the reaction and diffusion path, being a function of time and having a non-equilibrium character, can be represented and reasonably explained on the chemical potential diagram obtained from a thermodynamic treatment.

5. Conclusions

The interface reaction between $\mathrm{Cu_2O}$ and nickel for $\mathrm{Cu_2O}$ samples undoped and doped with NiO, has been investigated and the reaction path has been analysed on the chemical potential diagram for undoped and doped samples.

1. The layer sequences of products $\mathrm{Cu_2O}$/Cu/NiO/Ni for the undoped sample, and $\mathrm{Cu_2O}$/Cu/NiO/Cu–Ni alloy/Ni for the doped sample, were obtained.
2. The rate constant of product layers for the doped sample is higher than that for the undoped sample.
3. The content of nickel and oxygen in the copper phase for the doped sample was higher than that for the undoped sample.

Based on these facts, it is expected that the reaction and diffusion path of the doping sample passes a relatively higher point in the chemical potential of nickel in $\mathrm{Cu_2O}$ phase, higher in the chemical potentials of nickel and oxygen in the copper phase and at the Cu/NiO interface, and lower in the chemical potential of nickel NiO/Ni interface. The main difference of the reaction and diffusion path due to the doping is ascribed to a higher mobility of nickel and copper in the NiO phase. The reaction and diffusion path is represented approximately by the lines connected at the interface on the chemical potential diagram.

Acknowledgements

The author thanks Professor Masanori Kajihara, Tokyo Institute of Technology, for valuable discussions and comments. This work was done using the thermodynamic database “MALT2” compiled by the Society of Calorimetry and Thermal Analysis, Japan.

References

1. R. A. RAPP, A. EZIS and G. J. YUREK, *Metall. Trans.* **4** (1973) 1283
2. F. J. J. VAN LOO, *Prog. Solid State Chem.* **20** (1990) 47.
3. F. J. J. VAN LOO, J. A. VAN BEEK, G. F. BASTIN and R. METSELAAR, *Oxid. Metals* **22** (1984) 161.
4. M. BACKHAUS-RICOULT, H. SCHMALZRIED and R. J. TARENTO, *Ber. Bunsenges. Phys. Chem.* **95** (1991) 1593.
5. H. SCHMALZRIED, *J. Chem. Soc. Farad. Trans.* **86** (1990) 1273.
6. H. YOKOKAWA, T. KAWADA and M. DOKIYA, *J. Am. Ceram. Soc.* **72** (1989) 2104.
7. H. YOKOKAWA, N. SAKAI, T. KAWADA and M. DOKIYA, *J. Electrochem. Soc.* **138** (1991) 2719.
8. H. YOKOKAWA, N. SAKAI, T. KAWADA, M. DOKIYA and K. OHTA, *ibid.* **140** (1993) 3565.
9. M. BACKHAUS-RICOULT, *Ber. Bunsenges. Phys. Chem.* **90** (1986) 684.
10. C. WAGNER, *J. Electrochem. Soc.* **103** (1956) 571.
11. P. J. C. VOSTERS, M. A. J. TH. LAHEIJ, F. J. J. VAN LOOANK R. METSELAAR, *Oxid. Metals* **20** (1983) 147.

12. M. A. J. TH. LAHEIJ, F. J. J. VAN LOO and R. METSELAAR, *ibid.* **14** (1980) 207.
13. Y.-Z. YOO, K.-C. HSEIEH and Y. A. CHANG, *Metall. Trans.* **17A** (1986) 1104.
14. M. L. NARULA, V. B. TARE and W. L. WORRELL, *ibid.* **14B** (1983) 673.
15. R. GUAN, H. HASHIMOTO and K. H. KUO, *Acta Crystallogr.* **B46** (1990) 103.
16. J. S. KIRKALDY and D. J. YOUNG, "Diffusion in the Condensed State" (Institute of Metals, London, 1987).
17. J. S. KIRKALDY, *Can. J. Phys.* **36** (1958) 907.
18. *Idem, ibid.* **36** (1958) 917.
19. N. L. PETERSON and C. L. WILEY, *J. Phys. Chem. Solids* **46** (1985) 43.
20. K. HOSHINO and N. L. PETERSON, *ibid.* **45** (1984) 963.
21. C. MONTY, *Rad. Effects* **74** (1983) 29.

Received 15 June 1995
and accepted 2 July 1996